Cancer Chemotherapy and Pharmacology (2020) 85:251–263
https://doi.org/10.1007/s00280-019-04017-8

ORIGINAL ARTICLE

Prospective use of the single-mouse experimental design for the evaluation of PLX038A

Samson Ghilu[1] · Qilin Li[1] · Shaun D. Fontaine[2] · Daniel V. Santi[2] · Raushan T. Kurmasheva[1] · Siyuan Zheng[1] · Peter J. Houghton[1]

Received: 9 July 2019 / Accepted: 17 December 2019 / Published online: 11 January 2020

Abstract

Purpose Defining robust criteria for drug activity in preclinical studies allows for fewer animals per treatment group, and potentially allows for inclusion of additional cancer models that more accurately represent genetic diversity and, potentially, allows for tumor sensitivity biomarker identification.

Methods Using a single-mouse design, 32 pediatric xenograft tumor models representing diverse pediatric cancer types [Ewing sarcoma (9), brain (4), rhabdomyosarcoma (10), Wilms tumor (4), and non-CNS rhabdoid tumors (5)] were evaluated for response to a single administration of pegylated-SN38 (PLX038A), a controlled-release PEGylated formulation of SN-38. Endpoints measured were percent tumor regression, and event-free survival (EFS). The correlation between response to PLX038A was compared to that for ten models treated with irinotecan (2.5 mg/kg × 5 days × 2 cycles), using a traditional design (10 mice/group). Correlations between tumor sensitivity, genetic mutations and gene expression were sought. Models showing no disease at week 20 were categorized as 'extreme responders' to PLX038A, whereas those with EFS less than 5 weeks were categorized as 'resistant'.

Results The activity of PLX038A was evaluable in 31/32 models. PLX038A induced > 50% volume regressions in 25 models (78%). Initial tumor volume regression correlated only modestly with EFS ($r^2 = 0.238$), but sensitivity to PLX038A was better correlated with response to irinotecan when one tumor hypersensitive to PLX038A was omitted ($r^2 = 0.6844$). Mutations in *53BP1* were observed in three of six sensitive tumor models compared to none in resistant models ($n = 6$).

Conclusions This study demonstrates the feasibility of using a single-mouse design for assessing the antitumor activity of an agent, while encompassing greater genetic diversity representative of childhood cancers. PLX038A was highly active in most xenograft models, and tumor sensitivity to PLX038A was correlated with sensitivity to irinotecan, validating the single-mouse design in identifying agents with the same mechanism of action. Biomarkers that correlated with model sensitivity included wild-type *TP53*, or mutant *TP53* but with a mutation in *53BP1*, thus a defect in DNA damage response. These results support the value of the single-mouse experimental design.

Keywords Drug evaluation · Alternative experimental design · Single mouse study · Response criteria · Pediatric cancer · Genetic diversity

Introduction

The design of animal experiments to determine antitumor activity of a drug, or drug combination, is largely constrained by statistical considerations regarding the power to detect specific differences between control and treatment groups. This is in part determined by variance within the rate of growth of untreated controls, and the magnitude of the response to be detected. Greater variance between growths of control tumors necessitates increased numbers of animals to yield adequate statistical power, whereas increasing the

Electronic supplementary material The online version of this article (https://doi.org/10.1007/s00280-019-04017-8) contains supplementary material, which is available to authorized users.

✉ Peter J. Houghton
HoughtonP@uthscsa.edu

[1] Greehey Children's Cancer Research Institute, UT Health San Antonio, 8403 Floyd Curl Drive, San Antonio, TX 78229, USA

[2] ProLynx LLC, 455 Mission Bay Blvd, South San Francisco, CA 94158, USA

stringency of response criteria can have the opposite effect on group size. In preclinical studies, growth rates for tumors in treated animals are compared to those in controls, hence one can obtain data to show that treatment gives statistically significant differences (usually $P < 0.05$), although statistical significance does not imply a biologically meaningful effect. Tumor progression (> 25% increase in tumor volume) on treatment is a progressive disease in a clinical setting.

Clinical trial designs tend to use two endpoint criteria, tumor regression and progression-free survival (PFS). Response evaluation criteria in solid tumors (RECIST) sets out rules for evaluating when patients improve (respond), stay the same (stabilize) or worsen (progress) [1]. Statistical differences between experimental protocols are compared to an historical control arm, or more likely an alternative regimen, standard of care, or physician choice. One objective of preclinical experiments is to generate data that may accurately translate into the clinic. When considering how to assess antitumor activity when establishing the Pediatric Preclinical Testing Program (PPTP) it was considered that endpoint criteria should be similar between preclinical and clinical experiments [2]. In the ensuing 10 years where over 2100 tumor-drug evaluations were undertaken, it became clear that the great majority of drugs had relatively modest activity, or lacked activity, if these criteria were used. However, of greater concern was that using the standard design, based on the need to demonstrate 'statistical significance' relatively few models ($n = 6$–8) were used to represent a disease state (e.g., neuroblastoma). Genomics studies have revolutionized our understanding of histotype heterogeneity, with many pediatric cancers being classified into multiple subgroups based upon exome sequencing, expression profiles, etc. [3–9]. Thus, within resource constraints, it is reasonable to ask how one resolves the need to represent genetic heterogeneity, with considerations of statistical validity.

In a retrospective analysis of PPTP data that included 83 xenograft models, 67 drugs or biologics having different mechanisms of action, and over 2100 experiments, we found that the use of 1 mouse per treatment group would give the same result as the use of 10 mice (solid tumors) or 8 mice (acute leukemia models) in ~ 80% of experiments, and if small differences were allowed (partial response vs complete response [PR vs CR], for example) the predictive value of the single-mouse approach was ~ 95% [10].

Using conventional experimental designs, where group size is determined according to the variance in the rate of growth of tumors within a group and statistical endpoint being applied (for example, as described in [2]), necessitates use of large numbers of animals if relatively small drug effects are being sought. Thus, with finite resources, this necessarily restricts the number of models of any one cancer type that can be used. In the PPTP, six–eight models were used to represent each disease (e.g., osteosarcoma, neuroblastoma, etc.). Clearly, such a small number of models cannot accurately represent the genetic/epigenetic diversity of these cancer types. Thus, alternative approaches to preclinical in vivo testing need to be considered. We have proposed the use of a 'single-mouse' experimental design, where each mouse has a different patient derived xenograft, and endpoints are tumor regression and event-free survival (EFS). In this design, there is no control (untreated) tumor. Support for this idea comes from our retrospective study [10] that indicated use of one mouse per treatment group was adequate to identify agents that had activity and those that did not. If we consider control and treatment groups of ten mice each, the single-mouse design potentially allows inclusion of 20 models for every one used in conventional testing experiments.

Thus, the use of the single-mouse approach allows for the inclusion of more models of each pediatric cancer type, and hence increases the genetic heterogeneity potentially allowing identification of biomarkers of response that can be interrogated in a subsequent clinical trial. For example, assessing the activity of a drug against, say 30 tumors of one type (e.g., 30 medulloblastomas) may identify that drug sensitivity segregates with a particular set of genetic characteristics that may or may not be those shown to subclassify this disease [6, 11]. For example, preclinical testing in a large panel of adult melanoma xenografts shows that BRAF mutant models respond to BRAF inhibitors, whereas those with wild-type BRAF are less sensitive. Also, use of a larger number of models representative of a histotype may improve the prediction for activity in clinical trials [12].

Although the single-mouse approach is supported by the retrospective analysis of PPTP results, it has not been tested prospectively using pediatric cancer models. Here we have tested the feasibility of the single-mouse design to prospectively evaluate a long-acting PEGylated SN-38 prodrug, PLX038A, where SN-38 (the active metabolite of irinotecan) is released at a controlled rate [13, 14]. PLX038A was selected, as we have extensive recently derived data showing the activity of irinotecan in many of the same models using traditional testing design (ten mice/treatment and control groups); the conjecture being that xenograft models most sensitive to irinotecan would be the most sensitive to PLX038A, and conversely, tumors less sensitive to irinotecan would be less sensitive to PLX038A (i.e., validation of the ability of the single-mouse design to identify an agent where there is already data [from an analog] to indicate activity using conventional testing). Further, irinotecan has significant clinical activity, and is used in several high-risk and relapse protocols for treating childhood solid tumors [15, 16]. Other objectives of the study were to determine whether initial tumor volume regression correlated with EFS, and to mine the genomics data on each tumor model to identify potential biomarkers that relate to drug sensitivity.

Methods

The xenograft models used together with limited demographic data, where available, are presented in Table 1. Patient-derived xenografts (PDX; rhabdomyosarcomas Rh10, Rh18xe, Rh28, Rh30, Rh30R, Rh36, Rh41, Rh65; Wilms tumors KT5, KT10, KT11, KT13; and rhabdoid tumors KT12, KT14, KT16) and cell line-derived xenografts (Ewing sarcoma lines ES-1, ES-4, ES-6, EW-8, CHLA258, TC-71, SK-NEP-1; rhabdomyosarcomas SMS-CTR and Rh18c) have been described previously [2]. RBD-1 is an atypical teratoid rhabdoid tumor with *SMARB1* deletion, established as a PDX from a metastatic lung lesion, and the RBD-2 PDX was established from a liver mass. EW-5and NCH-EWS-1 are Ewing sarcoma PDXs from a paraspinal mass, and lung lesion, respectively. BT-35 and BT-40 brain tumors have been described

Table 1 Characteristics of pediatric xenograft models used

Histotype	Subtype	Gender	Age (years)	Tumor site	Status[a]
Ewing sarcoma					
ES-1	Type 1 t(11;22)	F	45	Thigh	Dx
ES-4	Type 1 t(11;22)	M	18	Pleura/lung	RL
ES-6	Type 1 t(11;22)	M	17	Fibula/BM	Rc
EW-5	Type 1 t(11;22)	M	16	Paraspinal	Post therapy
EW-8	Type 1 t(11;22)	M	17	Abdomen	Dx
NCH-EWS-1	No t(11;22) translocation	M	16	Lung	RL
CHLA258	Type 1 t(11;22)	F	14	Lung	RL
TC-71	Type 1 t(11;22)	M	22	Humerus	RL
SKNEP-1	Type 1 t(11;22)	F	25	Pleura	RL
Brain tumors					
BT-35	Anaplastic astrocytoma	M	12	Thalamus	Dx
BT-40*	JPA/anaplastic astrocytoma	M	14	Leptomeningeal	Dx
BT-39*	JPA/anaplastic astrocytoma	M	14	Leptomeningeal	Rc
S12-6321	Pleiomorphic xanthoastrocytoma	M	5	Right operculum	Rc
Rhabdomyosarcoma					
Rh10	Alveolar	F	15	Perineum	RL
Rh18c**	Embryonal	F	2	Perineum	Dx
Rh18xe**	Embryonal	F	2	Perineum	Dx
Rh28	Alveolar t(2;13)	M	17	Axillary node	
Rh30*	Alveolar t(2;13)	M	16	Bone marrow	Dx
Rh30R*	Alveolar t(2;13)	M	17	Bone marrow	RL
Rh36	Embryonal (HRAS Q61K)	M	15	Paratesticular	RL
Rh41	Alveolar t(2;13)	F	12	Liver	RL
Rh65	Alveolar t(2;13)	F	18	ND	RL
SMS-CTR	Embryonal (HRAS Q61K)	M	1	Pelvis	Dx
Kidney/ATRT cancers					
KT5	Wilms (NU)	M	6	Kidney	Dx
KT10	Wilms (FH)	M	6	Kidney	Dx
KT11	Wilms (FH)	F	4	Kidney	Dx
KT12	AT/RT	M	6	Ventricle	Dx
KT13	Wilms (DA)	F	3	Kidney/+ureter	Dx
KT14	AT/RT	F	16	Kidney	RL
KT16	AT/RT	F	10	Kidney	RL
RBD-1	AT/RT	ND	ND	Lung	
RBD-2	AT/RT	F	0.75	Liver	Dx

Dx diagnosis, *RL* relapse, *Rc* recurrent, *NU* nuclear unrest, *FH* favorable histology, *DA* diffuse anaplastic

*Same patient at Dx and Rc/RL

**Cell line derived from xenograft

[a]Patient status at the time the PDX was established

previously [17]. While BT-40 was originally described as a Juvenile Pilocytic Astrocytoma (JPA), it now resembles an anaplastic astrocytoma in mice. BT-39 was established at recurrence from the same patient as BT-40. S12-6321 was established from a patient with metastatic pleiomorphic xanthoastrocytoma [18]. All tumors were used at low passage and authenticated by STR analysis against reference profiles developed by this group. Tumor models were selected for testing without reference to genetic or molecular characteristics, or sensitivity to irinotecan in previous testing.

Evaluation in xenograft models

C.B.17SC scid −/− (C.B-Igh-1b/*IcrTac-Prkdcscid*) female mice (Envigo, Indianapolis, IN) were used to propagate subcutaneously implanted tumors as previously described [2]. All mice were maintained under barrier conditions and experiments were carried out using protocols and conditions approved by the institutional animal care and use committee of UTHSA. Mice were selected when tumors were 200–400 mm^3 (mean 297 ± 34 mm^3; range 260–370 mm^3). Methods similar to those developed in the Pediatric Preclinical Testing Program (PPTP) were used [2], only for these studies tumor volumes were measured for up to 20 weeks, and regrowth of tumors determined following tumor regression. Endpoints were time to event, defined as tumor growing to 400% of its volume at the initiation of treatment, (event-free survival (EFS), and percent tumor regression. Also recorded was the day where tumor could be detected following complete regression. Complete regression (CR; defined as tumor volume < 40 mm^3, the level of detection), and maintained CR (MCR) was defined as tumor volume < 40 mm^3 at week 20.

Formulation and treatment

PLX038A was provided as a solution in isotonic acetate buffer (pH 5.0; 143 mM NaCl, 20 mM NaOAc) and contained 8.2 mM SN-38 equivalents (2.1 mM conjugate; 4 equivalent SN-38 molecules/conjugate). Mice received a single administration of 120 µmol/kg (14.6 mL/kg; IP) when tumor volumes were 260–370 mm^3. Responses to PLX038A were compared to historical results for ten xenograft models treated with two cycles of irinotecan (2.5 mg/kg (days 1–5 and 21–25).

Pharmacokinetics

The synthesis and murine pharmacokinetics of PLX038A and PLX038 have been presented previously [19]. PLX038A was designed to mimic the human pharmacokinetics of PLX038 in mice. This optimization was required to compensate for the faster intrinsic clearance of PEG conjugates in mice. Since the $t_{1/2\beta}$ for PLX038 and PLX038A is 115 h (human) and 17 h (mouse), respectively, the rate of SN-38 release must be adjusted accordingly. A single administration of PLX038A (120 µmol/kg) was calculated to give adequate exposures of SN-38 over ~ 1 week.

Genomics analysis

DNA, RNA sequencing, Illumina BeadChip experiments were performed elsewhere [20] as part of the PPTC, according to the manufacturer-recommended protocols. Briefly, paired-end sequencing was performed on DNA samples by Baylor College of Medicine Human Genome Sequencing Center using Illumina cBot cluster generation system with TruSeq PE Cluster Generation Kits. Whole transcriptome RNA sequencing was performed using total RNA. For both DNA and RNA sequencing data, mouse reads were computationally removed before mutation calling and gene expression quantification. All high-level data have been described and are available on pedcbio portal (https://pedcbioportal.org/, under study "Pediatric Preclinical Testing Consortium").

Among the models tested, six were considered exceptional responders (MCR at 140 days) and six poor responders (EFS < 5 weeks) (Table 2). Mutation data for all 12 models were available and were compared with Fisher's exact test. Thresholded gene copy number matrix from GISTIC analysis [21] was used to identify genes with differential copy number status between the two groups for the 11 models that had copy number data available (excluding KT5). Fisher's exact test was applied similarly, followed by multiple testing adjustment with false discovery rate. Gene set enrichment analysis (GSEA) was used to compare pathway expression between the two groups [22] with five models in each. KT5 and RBD-1 did not have expression data, thus were excluded from this analysis.

Results

Selection of tumor models

The study had two main objectives: first, to determine the feasibility of the 'single-mouse experimental design' and second, whether this experimental design would identify tumor models with a spectrum of sensitivities to PLX038A that could reveal molecular characteristics associated with intrinsic sensitivity or resistance. Thus, models were selected where there were no prior data with irinotecan. However, as an approach to validating the single-mouse experimental design, we included 11 models where there were recently derived data for single agent irinotecan, but

Table 2 Genomic characteristics with respect to response to PLX038A

Response classification	EFS (days)	TP53 status	DDR gene coding mutations[a,b]	Other characteristics	
				ABCB1 FPKM[b]	ABCG2 FPKM
MCR at day 140					
Rh36	> 140	Wild type	53BP1 (P1565fs)	0	0.0058413
EW-8	> 140	Mutant (Y220C)	53BP1 (R1911K)	0	0.63868
KT5	> 140	Wild type		ND	ND
KT11	> 140	Wild type		0.322181	0.0122848
KT12	> 140	Wild type		0.0308	0.0971676
TC-71	> 140	Mutant (R213X)	53BP1 (M521L)	0.025247	0.217179
CR with recurrence by day 140					
SKNEP-1	38	Mutant (G245S)	FANCA (M415I)	0	0.00584
RBD-2	38	Wild type		0.11352	0.337757
Rh65	73	Wild type		0	0.0164548
NCH-EWS-1	59	Wild type		ND	ND
SMS-CTR	52	Mutant		ND	ND
Rh30	32	Wild type		0	0.0066162
KT10	38	Wild type	PALB2 (Y1108fs)	0.240029	0.0175957
KT16	140	Wild Type	BRCA1 (N810Y)	ND	ND
EFS < 5 weeks (poor responders)					
ES-1	24	Mutant		0	0.00516286
ES-4	24	Wild type		0	
Rh41	24	Mutant (p20-24del)		0.0401313	0.159367
RBD-1[c]	32	Wild type		ND	ND
S12-6321	32	Mutant (S183*)		27.6374	3.94092
Rh10	32	Wild type		0	0.00582257

ND not determined

[a]Data from the Pediatric Preclinical Testing Program (TARGET) or Pediatric Preclinical Testing Consortium (Maris) data sets deposited at https://pedcbioportal.org [26]

[b]FPKM, Fragments Per Kilobase of transcript per Million mapped reads, data from the Pediatric Preclinical Testing Program (TARGET) or Pediatric Preclinical Testing Consortium (Maris) data sets deposited at https://pedcbioportal.org [26]; DDR, DNA damage response genes

[c]Mt TP63(G541S)

using conventional testing (i.e., ten mice per treatment group). The underlying rationale was that if the 'single-mouse' data were valid there would be a correlation between model responsiveness to PLX038A with model responsiveness to irinotecan, a drug which has the same mechanism of action. Models used were selected independent of any molecular features. Characteristics of the 32 xenograft models are summarized in Table 1.

Evaluation of PLX038A

PLX038A was administered one time at a dose of 120 µmol/kg by intraperitoneal injection. Volume of tumors was determined on the day of treatment, and at 7-day intervals for a planned 20 weeks. There was one death: the mouse bearing Rh28 tumor died at day 21, probably not drug related. All data for Rh28 (both PLX038A and for irinotecan) have been excluded from analysis. Growth curves for each of the remaining 30 xenograft models are shown in the spider plot, Fig. 1. Only two models progressed without an initial shrinkage of volume, S12-6321 and Rh10. For tumors where PLX038A induced volume regression, the nadir occurred between day 7 and day 28 following drug administration (median day 7). Thirteen models regressed to below the level of detection (~ 40 mm^3; 100% regression), with 12 additional models meeting criteria for partial response (≥ 50% volume regression but > 40 mm^3), as shown in the 'waterfall' plot, Fig. 2a. Six models showed no disease at 20 weeks (Rh36, EW8, KT5, KT11, KT12 and TC-71). At week 20, KT16 xenografts were measurable, but had not reached event at time of terminating the experiment (week 20), shown in the 'swimmer plot', Fig. 2b. There were eight models where EFS was < 5 weeks (ES1, ES4, CHLA258, Rh10, Rh30, Rh41, RBD-1 and S12-6321).

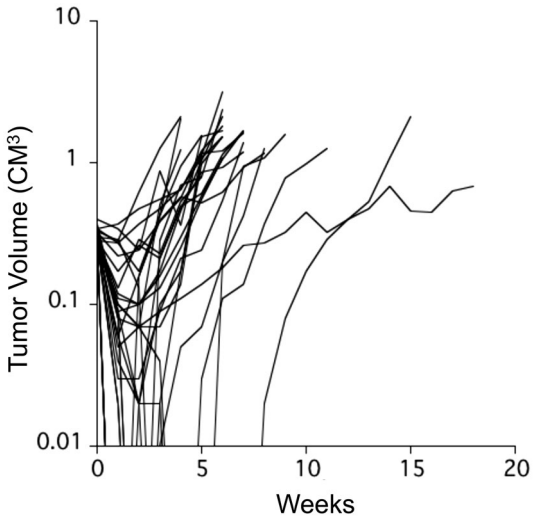

Fig. 1 Responses of 31 individual xenograft models in mice treated with a single administration of PLX038A. Tumor diameters were measured weekly until tumor reached endpoint criteria (fourfold volume at day of treatment) or day 140 when experiments were terminated

Endpoint criteria: tumor regression vs EFS

Clinical criteria used in RECIST assessment use tumor regression and time to event as indicative of antitumor activity of an agent/regimen. Clearly, a single administration of PLX038A was effective at causing regression of most tumor models. However, how relevant initial regression is to outcome (EFS) is less clear ($r^2 = 0.2293$). The relationship between initial tumor regression and EFS is shown in Fig. 2c. Tumors that had the greatest regression (i.e. 100%) tended to have the greatest EFS; however, the relationship is complex with some models regressing completely, but recurring rapidly and having relatively short EFS. For 13 tumors that regressed below the level of detection, the range of EFS was from 38 to > 140 days, and time to first detection of tumor following CR ranged from 14 to > 140 days. For eight xenograft models that had CR but recurred, the time to event from the first detection of recurrent tumor ranged from 9 days (SMS-CTR) to 46 days KT10, (median 25 days), indicating a range of regrowth rates, independent of the initial response to PLX038A.

Tumor sensitivity to PLX038A vs irinotecan

PLX038A is a controlled release form of SN-38, the active metabolite of irinotecan; hence, both agents have the same mechanism of action, although very different pharmacokinetics [19]. We, therefore, sought to determine whether there was a correlation between the responses to each agent within the panel of tumors used for the single-mouse experiment and in a subset of ten tumor models where evaluation of irinotecan used conventional testing (ten mice per treatment group). In these studies, irinotecan had been administered at 2.5 mg/kg daily for 5 days, with the cycle repeated at day 21. This dose of irinotecan generates SN-38 exposures relevant to exposure in children administered 50 mg/m^2 daily for 5 days in each cycle of treatment. As shown in Fig. 3a, there is a correlation between the event-free survival for irinotecan [EFS(IRN)] and that induced by PLX038A [EFS(PLX038A)]; however, the relationship is somewhat obscured by the very high EFS induced by PLX038A in the KT11 (Wilms tumor) model. Removing the KT11 'outlier' improved the correlation coefficient (Fig. 3b; $r^2 = 0.6844$).

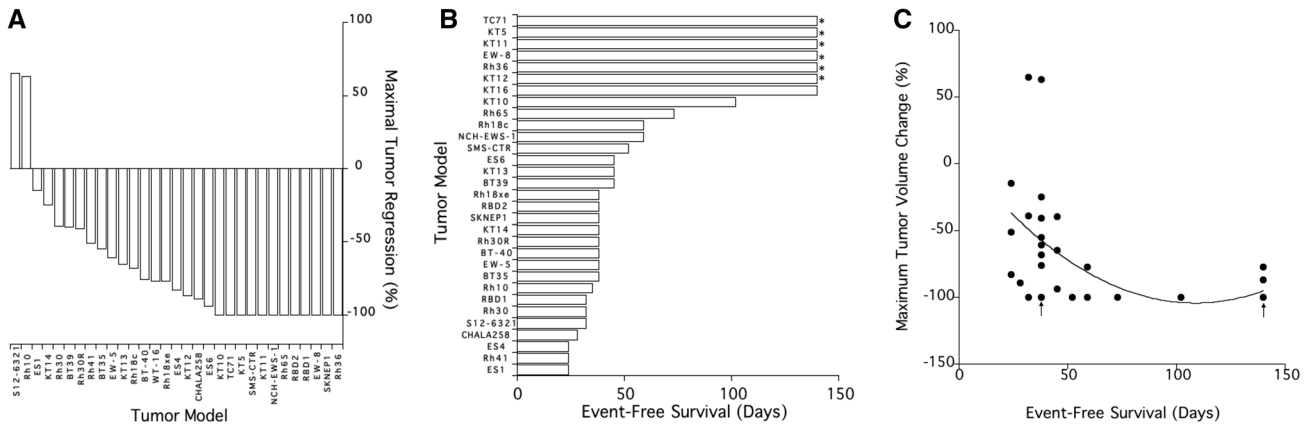

Fig. 2 **a** 'Waterfall' plot showing the maximal tumor volume regression (100% is a volume below level of detection ~40 mm^3) in mice treated with a single administration of PLX038A; **b** "Swimmer' plot showing the EFS for 31 xenograft models in treated xenografts. Tumors marked with an asterisk are those where there was no detectable tumor at termination of the experiment at day 140. **c** The relationship between the maximal tumor volume reduction and EFS for 31 xenograft models in mice treated with PLX038A ($r^2 = 0.2293$). Arrows mark overlapping coordinates for SK-NEP-1 and RBD-2 [day 38] and Rh36, EW-8, TC-71, KT5 and KT11 [day 140])

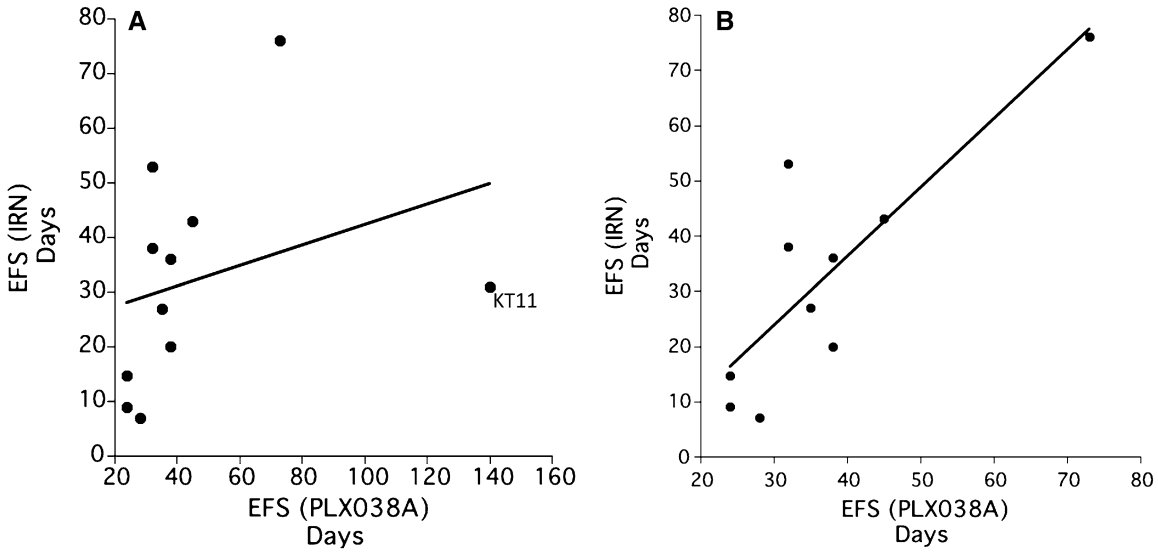

Fig. 3 **a** The relationship between EFS determined after irinotecan [2.5 mg/kg daily × 5; EFS(IRN)] and EFS following a single administration of PLX038A (EFS[PLX038A]). KT11 xenografts are identified as an outlier sensitive to PLX038A. Data for irinotecan are median EFS for groups of 10 treated mice; **b** the same data without KT11 ($r^2 = 0.6844$)

Molecular correlates with sensitivity

The 'single-mouse' experimental approach potentially offers an advantage of allowing evaluation of a drug against a large panel of models within any particular cancer histology, or between histology's, facilitating the potential to identify 'extreme responders' that may be valuable in identifying biomarkers of drug sensitivity or resistance. Within the panel of xenografts, six models had EFS > 140 days (exceptional responders) and conversely, six models where EFS was less than 5 weeks (intrinsically resistant models). We did not observe any gene that demonstrated significant copy number differences between the two groups. However, we found p53 binding protein 1 (*53BP1*) nonsynonymous mutations (two missense and one frame-shift) in 3 of the 6 models that remained in CR at day 140, compared to none in the six tumors with an EFS less than 5 weeks (*P* value 0.18, Fisher's exact test; Table 2). Among the three mutants, two (EW8 and TC-71) have mutated *TP53* whereas *TP53* is wild type in four models (Rh36, KT5, KT11, KT12). The other two top differentially mutated genes were NPHP4 and HMCN1, both had mutations in three responder cases but none in six resistant models (Fig. 4).

We next compared gene expression of resistant and sensitive models. KT5 from the sensitive group and RBD-1 from the resistant group were dropped due to lack of expression data. Gene Set Enrichment Analysis (GSEA) revealed DNA mismatch repair and replication pathways were upregulated in the resistant group with borderline statistical significance (nominal *P* values 0.08 and 0.15, respectively) (Supplementary Fig. 1), corroborating

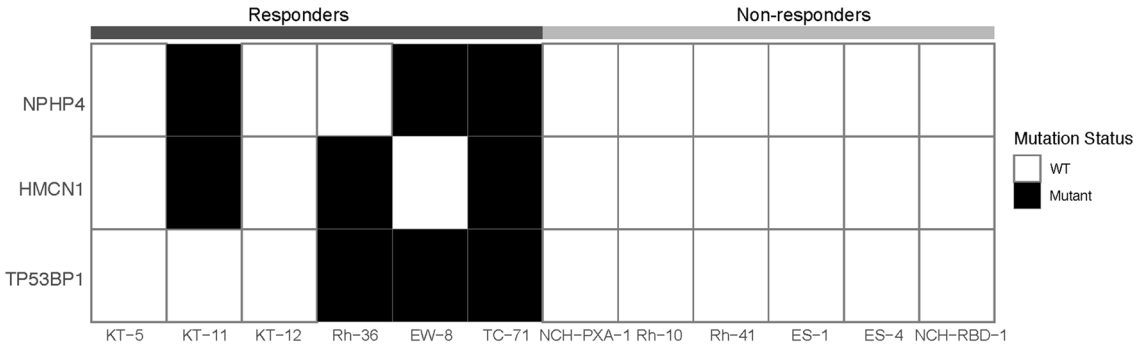

Fig. 4 Differentially mutated genes between resistant and sensitive tumors. Solid black cell indicates a non-synonymous mutation. The three genes shown in the heatmap have the most significant *P* values ($P = 0.18$) from Fisher's exact test without reaching statistical significance

the observation from mutation data that DNA damage response might be a marker for responses to PLX038A.

There were nine models where PLX038A induced a CR, but where tumors recurred within the 120-day period of observation. Of these only two (SMS-CTR [23], SKNEP-1) have mutant *TP53*; SKNEP-1 also has a potentially deleterious mutation in *FANCA* (M415I). SMS-CTR was not sequenced as part of the PPTC effort. The *TP53* status for SMS-CTR has not been determined. The other seven models have wild-type *TP53*.

The drug transporters, *ABCB1*, which encodes P-glycoprotein, and *ABCG2*, which encodes BCRP, have both been implicated in resistance to camptothecin drugs [24, 25]. Hence, it was of interest to determine whether the levels of expression of these transporters correlated with intrinsic sensitivity or resistance of the tumor models to PLX038A. Expression (mRNA) of these transporters was available for 14 models (Table 2) from the Pediatric Preclinical Testing Consortium (PPTC) database: https://pedcbioportal.org [26]. Of interest, with one exception (S12-6321), expression of both transporters was very low or not detected, irrespective of the sensitivity of the tumor model to PLX038A. For *ABCB1*, levels ranged from 0.00 to 0.322 FPKM and for *ABCG2*, from 0.00516 to 0.6387 FPKM. In contrast, for S12-6321, mRNA levels for *ABCB1* and *ABCG2* were 27.637 FPKM and 3.940 FPKM, respectively.

Discussion

Compared to adult cancers, most pediatric malignancies have very few coding mutations [27]. However, genomic and other molecular profiling has revealed the molecular heterogeneity of many pediatric cancers. Thus, while the mutation load for pediatric cancers is low in terms of coding mutations per Mb, pediatric cancers are driven by a range of molecular aberrations, and it is estimated that nearly 50% harbor a potentially druggable event [27]. For neuroblastoma, a subset of patients have *ALK* mutations that drive the genesis of disease that can be targeted by *ALK* inhibitors [28, 29], and mutations in the *RAS* pathway are more frequent at relapse following chemotherapy [30]. For pediatric brain tumors, medulloblastoma can be classed into four main subgroups based upon molecular characterization [6]. One subgroup is characterized by activation of the sonic hedgehog pathway, and some patients have benefitted from treatment with smoothened inhibitors; however, not all patients respond [31]. Low-grade glioma (LGG), the most frequent brain tumor in children, is characterized by aberrant *BRAF* signaling, and drugs such as selumetinib or dabrafenib have significant clinical activity [32–34]. However, in the phase II trial of selumetinib, while very few patients with either BRAF-driven LGG of NF1-driven neurofibromatosis progressed on treatment, only 40% achieved criteria for partial response. Hence, even with druggable aberrations, there is a diversity of responses that may be conferred by additional mutations or epigenetic changes that are currently not understood. Other frequently occurring genetic changes are anaplasia and T*P53* mutations mark high-risk Wilms tumors [35, 36] and *RAS* mutations characterize most of the high-risk embryonal rhabdomyosarcomas [3]. Consequently, at a preclinical level, to adequately represent any clinical entity with reasonable expectation of including its genetic diversity requires generation of many preclinical models.

The experience in adult oncology trials of BRAF or MEK inhibitors in BRAF-mutant melanoma or colon carcinoma demonstrates that factors other than the driving mutation may influence response to therapy [37, 38]. Hence, accurately modeling these diseases may be valuable in identifying effective therapeutic combinations, or molecular characteristics that accurately predict patient response to therapeutics. However, to model the heterogeneity of any clinical disease will require establishment of adequate models, and an experimental design that can accommodate testing. The number of models required to represent a clinical entity will be dependent on the genetic heterogeneity, and the NCI-supported PDXNet is an attempt to generate and characterize a large number of patient-derived xenografts, organoid and 3D culture lines (https://www.pdxnetwork.org). For pediatric cancers that lack the genetic instability that characterizes many adult malignancies, the numbers of models to represent a disease entity may be smaller, although it is important to model tumor at diagnosis and also relapse.

Recent changes in regulatory statutes under the Research to Accelerate Cures and Equity for Children Act (RACE for Children Act), part of the FDA Reauthorization Act (FDARA), require FDA to develop a list of molecular targets and molecular targets of new drugs and biologics in development that are determined to be substantially relevant to the growth and progression of pediatric cancer, and that may trigger the requirement for pediatric investigations. The intent is to engage Pharma in pediatric testing at an earlier stage in drug development (https://www.fda.gov/about-fda/oncology-center-excellence/pediatric-oncology). As discussed above, all tumors having a similar molecular characteristic (e.g., BRAFV600E or ALK mutation) do not respond equally, and this was clearly demonstrated in the recent phase II evaluation of the MEK inhibitor, selumetinib, in pediatric low-grade glioma [34]. Thus, many PDXs may be required to accurately recapitulate the clinical heterogeneity/drug responsiveness in diseases that exhibit the characteristics identified by FDA. Testing using conventional experimental designs will undoubtedly strain current testing resources; hence, the use of the single-mouse design, presented here, offers one potential solution.

Researchers at Novartis first proposed using multiple models of melanoma in individual mice as a preclinical approach to simulating clinical diversity [12]. Our retrospective analysis of 10 years of screening for the PPTP indicated that with a few exceptions, models would give similar data whether one or ten mice per treatment group (for solid tumors or eight mice per treatment group for leukemias) were used [10]. In this retrospective study, the single mouse accurately predicted group median response in 78% of experiments, and if one allowed a deviation of one response classification, the prediction success was ~95%.

To test the feasibility and validity of the single-mouse experimental design, we prospectively evaluated a PEGylated-SN38 polymer that releases SN-38 at a controlled rate and potentially has greater selectivity through enhanced permeability and retention (EPR) properties [39, 40]. The single-mouse data was compared to a data set derived using ten mice per group that evaluated irinotecan (2.5 mg/kg daily × 5 with treatment repeated at days 21–25) in a subset of models common to both studies. The antitumor activity of both agents is via SN-38-generated poisoning of topoisomerase I, and generation of DNA single- and double-strand breaks [41, 42]; thus, it was anticipated that there would be a correlation between responses of tumors to both agents, if the single-mouse design was accurate. However, as the dosing or exposures to irinotecan were different from PLX038A, it was not anticipated that the results from the two agents would be the same in terms of tumor regression or EFS. We compared ten models where there were data for irinotecan and PLX038A. Only one tumor model was an outlier (KT11), in that it was far more sensitive to PLX038A than to irinotecan. By omitting KT11 from the analysis, the relationship between EFS induced by either drug improved ($r^2 = 0.6844$).

Camptothecin-based topoisomerase I poisons are effective in the treatment of some pediatric sarcomas [15, 43], Wilms tumor [44] and other childhood malignancies [45] alone, or in combination with other cytotoxic agents [15, 43, 46, 47]; thus, the marked antitumor activity of PLX038A was anticipated. The pediatric cancer models used in this study were highly volume responsive to PLX038A; hence, this gave an opportunity to determine whether initial response, in terms of tumor regression, correlated with EFS. Put another way, could initial volume response be used to predict outcome (EFS). Although there is a relationship, it is relatively poor, with EFS ranging from 38 to 140 days for tumors that initially regressed below the volume for detection. This discordance does not appear to be caused by the intrinsic rate of growth of each tumor model, based on EFS times for control tumors in the irinotecan cohort. This raises the question as to which endpoint is most valuable to use in preclinical studies. Clearly, with these volume-responsive tumor models, there is a poor relationship between volume regression and EFS that is largely independent of tumor growth rate. This may be a consequence of inadequate sensitivity for tumor measurements, as volume measurements do not accurately reflect log cell kill. We have defined EFS as the time at which a tumor reaches fourfold the volume at the beginning of treatment. This metric can be used whether a tumor regresses or progresses on treatment. An alternative would be to assess time to progression (PFS, i.e., the day when tumor becomes measurable) for tumors where there is CR of disease following treatment. However, the advantage of EFS over PFS is that with EFS, there is a period for continued tumor growth measurement that gives confidence that this is tumor recurrence, and not detection of some fibrotic tissue at the site of the original tumor. Determining EFS is also valuable for calculating log cell kill induced by treatment [48], although the single-mouse experimental design does not have a 'control' from which to calculate growth rate. However, for models that have consistent growth characteristics, growth rates from historical cohorts may prove adequate.

The single-mouse experimental design allows for a large number of tumors to be evaluated; hence, offers an opportunity to relate molecular features in characterized tumor models with drug sensitivity. In the current study, we used baseline genomic and expression profiles derived from PDX models that were derived at different stages of disease and treatment (diagnosis, recurrence, relapse) sequenced as part of the Pediatric Preclinical Testing Consortium (PPTC). Thus, in these tumors, mutations and gene expression profiles represent those in the control situation for the current therapeutic study (i.e., these data were derived before PLX038A or irinotecan treatment in mice). We were able to identify six xenograft models where EFS was less than 5 weeks (intrinsically resistant) and six exceptional responders (EFS > 140 days) using the uniform clinical end points, and eventually compared tumors from ten models for genomic correlates with response to PLX038A. While the number was still too small to pinpoint the molecular feature associated with drug sensitivity, our results suggested the mouse models we used can recapitulate drug response phenotypes from histology or even other topoisomerase inhibitors evidenced by the identification of genes implicated in driving distinct responses to this class of agents.

In this study, we used models representing several histology's (sarcoma, brain tumors, Wilms/rhabdoid) to demonstrate the feasibility of conducting single-mouse studies. We speculate that the single-mouse model design is a key as it allows for the inclusion of tumors with different histology thus effectively minimizes confounding tissue effects. Alternatively, conducting such studies utilizing, say, thirty RAS-mutant embryonal rhabdomyosarcomas may reveal a range of sensitivities to MAPK inhibitors, and allow a greater understanding of associated genetic/epigenetic change that correlate with tumor sensitivity. Results presented here raise

a testable hypothesis that p53-binding protein 1 (*53BP1*) inactivating mutations are a useful biomarker for responses to PLX038A. In support of this contention, it is known that 53BP1 is involved in hyperphosphorylation of replication protein A (RPA2) following DNA damage, and inhibition of 53BP1 function can sensitize cells to topoisomerase I poisons such as camptothecin [49]. Further investigation of *53BP1*-mediated DNA damage repair and PLX038A-induced cell death may provide new insights into how these two pathways are interlinked and how this interaction can be exploited clinically.

Preclinical studies identified irinotecan as an active agent for treatment of several pediatric solid tumors [50, 51], and that antitumor activity was optimal when irinotecan was administered over a protracted period. Currently, for pediatric indications, clinical administration of irinotecan is by short infusion daily for 5 days at 50 mg/m^2/day (Children's Oncology Group), or for 5 days on two consecutive weeks at 20 mg/m^2/day (St. Jude schedule). Alternatively, irinotecan is administered orally for five consecutive days at 90 mg/m^2, the higher dose reflecting the poor oral bioavailability of irinotecan both in mice and patients [52, 53]. In contrast, PLX038 is administered by infusion over 60 min every 21 days, hence would be advantageous in terms of patient convenience and cost.

Following a single dose of PLX038A, 13 models (43%) were in PR (7) or CR (6) at week 3 following a single dose of PLX038A, and only four models (13%) had progressed (> 25% increase in tumor volume), with other tumor models representing stable disease (SD; < 25% progression, < 50% regression). Thus, 87% of models would have been eligible for further treatment if representing a patient in a clinical context. A comparison of the activity of PLX038A and cycle 1 of irinotecan was available for 11 models. For PLX038A treatment, 7 (63%) had not progressed by day 21, hence would meet criteria for a second cycle of treatment. Analysis of the day-21 status of tumors in the cohort treated with irinotecan (2.5 mg/kg daily × 5), prior to starting a second cycle of irinotecan therapy, shows that 6/11 (54%) models had progressed (> 25% increase in tumor volume over day 1 of treatment), whereas five models (45%) had PR/CR. Thus, using 'clinical' criteria, in the cohort of 11 models with data from both treatments, mice bearing 63% of models would qualify for at least one further treatment with PLX038A, whereas following one cycle of irinotecan only 45% would meet criteria for treatment with cycle 2.

Future development of PLX038 may well be dependent on the demonstration of tolerability and activity in adult patients. Results presented here indicate that PLX038A in mice is highly active, and equal to or slightly superior to a single cycle of irinotecan. While it is accepted that mouse models can overpredict for activity in a clinical setting, irinotecan and PLX038A have the same mechanism of action; hence, it would be anticipated that PLX038 would have activity against many pediatric cancers shown to be responsive to irinotecan. Future development in a pediatric setting would probably involve combining PLX038 with vincristine, as an effective combination, as well as with radiation therapy. Further preclinical studies testing such combinations may be valuable in advancing this agent to pediatric clinical trials.

Funding This work was funded in part by USPHS award UO1CA199297, CA169368 and CA165995 (PJH) from NCI and CPRIT PR170055 (SZ).

Compliance with ethical standards

Conflict of interest S. Ghilu declares that he has no conflict of interest. Q. Li declares that he has no conflict of interest. S. D. Fontaine is an employee and holds stock in Prolynx. D. V. Santi is an employee and holds stock in Prolynx. R. T. Kurmasheva declares that she has no conflict of interest. S. Zheng declares that he has no conflict of interest. P. J. Houghton declares that he has no conflict of interest.

Ethical approval All applicable international, national, and/or institutional guidelines for the care and use of animals were followed. This article does not contain any studies with human participants.

References

1. Eisenhauer EA, Therasse P, Bogaerts J, Schwartz LH, Sargent D, Ford R, Dancey J, Arbuck S, Gwyther S, Mooney M, Rubinstein L, Shankar L, Dodd L, Kaplan R, Lacombe D, Verweij J (2009) New response evaluation criteria in solid tumours: revised RECIST guideline (version 1.1). Eur J Cancer 45(2):228–247. https://doi.org/10.1016/j.ejca.2008.10.026
2. Houghton PJ, Morton CL, Tucker C, Payne D, Favours E, Cole C, Gorlick R, Kolb EA, Zhang W, Lock R, Carol H, Tajbakhsh M, Reynolds CP, Maris JM, Courtright J, Keir ST, Friedman HS, Stopford C, Zeidner J, Wu J, Liu T, Billups CA, Khan J, Ansher S, Zhang J, Smith MA (2007) The pediatric preclinical testing program: description of models and early testing results. Pediatr Blood Cancer 49(7):928–940. https://doi.org/10.1002/pbc.21078
3. Shern JF, Chen L, Chmielecki J, Wei JS, Patidar R, Rosenberg M, Ambrogio L, Auclair D, Wang J, Song YK, Tolman C, Hurd L, Liao H, Zhang S, Bogen D, Brohl AS, Sindiri S, Catchpoole D, Badgett T, Getz G, Mora J, Anderson JR, Skapek SX, Barr FG, Meyerson M, Hawkins DS, Khan J (2014) Comprehensive genomic analysis of rhabdomyosarcoma reveals a landscape of alterations affecting a common genetic axis in fusion-positive and fusion-negative tumors. Cancer Discov 4(2):216–231. https://doi.org/10.1158/2159-8290.CD-13-0639
4. Brohl AS, Solomon DA, Chang W, Wang J, Song Y, Sindiri S, Patidar R, Hurd L, Chen L, Shern JF, Liao H, Wen X, Gerard J, Kim JS, Lopez Guerrero JA, Machado I, Wai DH, Picci P, Triche T, Horvai AE, Miettinen M, Wei JS, Catchpool D, Llombart-Bosch A, Waldman T, Khan J (2014) The genomic landscape of the Ewing Sarcoma family of tumors reveals recurrent STAG2 mutation. PLoS Genet 10(7):e1004475. https://doi.org/10.1371/journal.pgen.1004475

5. Hwang EI, Kool M, Burger PC, Capper D, Chavez L, Brabetz S, Williams-Hughes C, Billups C, Heier L, Jaju A, Michalski J, Li Y, Leary S, Zhou T, von Deimling A, Jones DTW, Fouladi M, Pollack IF, Gajjar A, Packer RJ, Pfister SM, Olson JM (2018) Extensive molecular and clinical heterogeneity in patients with histologically diagnosed CNS-PNET treated as a single entity: a report from the children's oncology group randomized ACNS0332 trial. J Clin Oncol. https://doi.org/10.1200/JCO.2017.76.4720
6. Kool M, Korshunov A, Remke M, Jones DT, Schlanstein M, Northcott PA, Cho YJ, Koster J, Schouten-van Meeteren A, van Vuurden D, Clifford SC, Pietsch T, von Bueren AO, Rutkowski S, McCabe M, Collins VP, Backlund ML, Haberler C, Bourdeaut F, Delattre O, Doz F, Ellison DW, Gilbertson RJ, Pomeroy SL, Taylor MD, Lichter P, Pfister SM (2012) Molecular subgroups of medulloblastoma: an international meta-analysis of transcriptome, genetic aberrations, and clinical data of WNT, SHH, group 3, and group 4 medulloblastomas. Acta Neuropathol 123(4):473–484. https://doi.org/10.1007/s00401-012-0958-8
7. Pajtler KW, Witt H, Sill M, Jones DT, Hovestadt V, Kratochwil F, Wani K, Tatevossian R, Punchihewa C, Johann P, Reimand J, Warnatz HJ, Ryzhova M, Mack S, Ramaswamy V, Capper D, Schweizer L, Sieber L, Wittmann A, Huang Z, van Sluis P, Volckmann R, Koster J, Versteeg R, Fults D, Toledano H, Avigad S, Hoffman LM, Donson AM, Foreman N, Hewer E, Zitterbart K, Gilbert M, Armstrong TS, Gupta N, Allen JC, Karajannis MA, Zagzag D, Hasselblatt M, Kulozik AE, Witt O, Collins VP, von Hoff K, Rutkowski S, Pietsch T, Bader G, Yaspo ML, von Deimling A, Lichter P, Taylor MD, Gilbertson R, Ellison DW, Aldape K, Korshunov A, Kool M, Pfister SM (2015) Molecular classification of ependymal tumors across all CNS compartments, histopathological grades, and age groups. Cancer Cell 27(5):728–743. https://doi.org/10.1016/j.ccell.2015.04.002
8. Oberthuer A, Hero B, Berthold F, Juraeva D, Faldum A, Kahlert Y, Asgharzadeh S, Seeger R, Scaruffi P, Tonini GP, Janoueix-Lerosey I, Delattre O, Schleiermacher G, Vandesompele J, Vermeulen J, Speleman F, Noguera R, Piqueras M, Benard J, Valent A, Avigad S, Yaniv I, Weber A, Christiansen H, Grundy RG, Schardt K, Schwab M, Eils R, Warnat P, Kaderali L, Simon T, Decarolis B, Theissen J, Westermann F, Brors B, Fischer M (2010) Prognostic impact of gene expression-based classification for neuroblastoma. J Clin Oncol 28(21):3506–3515. https://doi.org/10.1200/JCO.2009.27.3367
9. Oberthuer A, Juraeva D, Hero B, Volland R, Sterz C, Schmidt R, Faldum A, Kahlert Y, Engesser A, Asgharzadeh S, Seeger R, Ohira M, Nakagawara A, Scaruffi P, Tonini GP, Janoueix-Lerosey I, Delattre O, Schleiermacher G, Vandesompele J, Speleman F, Noguera R, Piqueras M, Benard J, Valent A, Avigad S, Yaniv I, Grundy RG, Ortmann M, Shao C, Schwab M, Eils R, Simon T, Theissen J, Berthold F, Westermann F, Brors B, Fischer M (2015) Revised risk estimation and treatment stratification of low- and intermediate-risk neuroblastoma patients by integrating clinical and molecular prognostic markers. Clin Cancer Res 21(8):1904–1915. https://doi.org/10.1158/1078-0432.CCR-14-0817
10. Murphy B, Yin H, Maris JM, Kolb EA, Gorlick R, Reynolds CP, Kang MH, Keir ST, Kurmasheva RT, Dvorchik I, Wu J, Billups CA, Boateng N, Smith MA, Lock RB, Houghton PJ (2016) Evaluation of alternative in vivo drug screening methodology: a single mouse analysis. Cancer Res 76(19):5798–5809. https://doi.org/10.1158/0008-5472.CAN-16-0122
11. Northcott PA, Dubuc AM, Pfister S, Taylor MD (2012) Molecular subgroups of medulloblastoma. Expert Rev Neurother 12(7):871–884. https://doi.org/10.1586/ern.12.66
12. Gao H, Korn JM, Ferretti S, Monahan JE, Wang Y, Singh M, Zhang C, Schnell C, Yang G, Zhang Y, Balbin OA, Barbe S, Cai H, Casey F, Chatterjee S, Chiang DY, Chuai S, Cogan SM, Collins SD, Dammassa E, Ebel N, Embry M, Green J, Kauffmann A, Kowal C, Leary RJ, Lehar J, Liang Y, Loo A, Lorenzana E, Robert McDonald E 3rd, McLaughlin ME, Merkin J, Meyer R, Naylor TL, Patawaran M, Reddy A, Roelli C, Ruddy DA, Salangsang F, Santacroce F, Singh AP, Tang Y, Tinetto W, Tobler S, Velazquez R, Venkatesan K, Von Arx F, Wang HQ, Wang Z, Wiesmann M, Wyss D, Xu F, Bitter H, Atadja P, Lees E, Hofmann F, Li E, Keen N, Cozens R, Jensen MR, Pryer NK, Williams JA, Sellers WR (2015) High-throughput screening using patient-derived tumor xenografts to predict clinical trial drug response. Nat Med 21(11):1318–1325. https://doi.org/10.1038/nm.3954
13. Santi DV, Schneider EL, Ashley GW (2014) Macromolecular prodrug that provides the irinotecan (CPT-11) active-metabolite SN-38 with ultralong half-life, low C(max), and low glucuronide formation. J Med Chem 57(6):2303–2314. https://doi.org/10.1021/jm401644v
14. Santi DV, Schneider EL, Reid R, Robinson L, Ashley GW (2012) Predictable and tunable half-life extension of therapeutic agents by controlled chemical release from macromolecular conjugates. Proc Natl Acad Sci USA 109(16):6211–6216. https://doi.org/10.1073/pnas.1117147109
15. Pappo AS, Lyden E, Breitfeld P, Donaldson SS, Wiener E, Parham D, Crews KR, Houghton P, Meyer WH, Children's Oncology G (2007) Two consecutive phase II window trials of irinotecan alone or in combination with vincristine for the treatment of metastatic rhabdomyosarcoma: the children's oncology group. J Clin Oncol 25(4):362–369. https://doi.org/10.1200/JCO.2006.07.1720
16. Weigel BJ, Lyden E, Anderson JR, Meyer WH, Parham DM, Rodeberg DA, Michalski JM, Hawkins DS, Arndt CA (2016) Intensive multiagent therapy, including dose-compressed cycles of ifosfamide/etoposide and vincristine/doxorubicin/cyclophosphamide, irinotecan, and radiation, in patients with high-risk rhabdomyosarcoma: a report from the children's oncology group. J Clin Oncol 34(2):117–122. https://doi.org/10.1200/JCO.2015.63.4048
17. Kolb EA, Gorlick R, Houghton PJ, Morton CL, Neale G, Keir ST, Carol H, Lock R, Phelps D, Kang MH, Reynolds CP, Maris JM, Billups C, Smith MA (2010) Initial testing (stage 1) of AZD6244 (ARRY-142886) by the pediatric preclinical testing program. Pediatr Blood Cancer 55(4):668–677. https://doi.org/10.1002/pbc.22576
18. Saraf AJ, Elhawary G, Finlay JL, Scott S, Olshefski R, Halverson M, Boue DR, AbdelBaki MS (2018) Complete remission of an extracranially disseminated anaplastic pleomorphic xanthoastrocytoma with everolimus: a case report and literature review. Pediatr Neurol 88:65–70. https://doi.org/10.1016/j.pediatrneurol.2018.09.004
19. Fontaine SD, Hann B, Reid R, Ashley GW, Santi DV (2019) Species-specific optimization of PEG~SN-38 prodrug pharmacokinetics and antitumor effects in a triple-negative BRCA1-deficient xenograft. Cancer Chemother Pharmacol 84(4):729–738. https://doi.org/10.1007/s00280-019-03903-5
20. Rokita JL, Rathi KS, Cardenas MF, Upton KA, Jayaseelan J, Cross KL, Pfeil J, Egolf LE, Way GP, Farrel A, Kendsersky NM, Patel K, Gaonkar KS, Modi A, Berko ER, Lopez G, Vaksman Z, Mayoh C, Nance J, McCoy K, Haber M, Evans K, McCalmont H, Bendak K, Bohm JW, Marshall GM, Tyrrell V, Kalletla K, Braun FK, Qi L, Du Y, Zhang H, Lindsay HB, Zhao S, Shu J, Baxter P, Morton C, Kurmashev D, Zheng S, Chen Y, Bowen J, Bryan AC, Leraas KM, Coppens SE, Doddapaneni H, Momin Z, Zhang W, Sacks GI, Hart LS, Krytska K, Mosse YP, Gatto GJ, Sanchez Y, Greene CS, Diskin SJ, Vaske OM, Haussler D, Gastier-Foster JM, Kolb EA, Gorlick R, Li XN, Reynolds CP, Kurmasheva RT, Houghton PJ, Smith MA, Lock RB, Raman P, Wheeler DA, Maris JM (2019) Genomic profiling of childhood tumor patient-derived xenograft models to enable rational clinical trial design. Cell Rep 29(6):1675–1689. https://doi.org/10.1016/j.celrep.2019.09.071

21. Mermel CH, Schumacher SE, Hill B, Meyerson ML, Beroukhim R, Getz G (2011) GISTIC2.0 facilitates sensitive and confident localization of the targets of focal somatic copy-number alteration in human cancers. Genome Biol 12(4):R41. https://doi.org/10.1186/gb-2011-12-4-r41
22. Subramanian A, Tamayo P, Mootha VK, Mukherjee S, Ebert BL, Gillette MA, Paulovich A, Pomeroy SL, Golub TR, Lander ES, Mesirov JP (2005) Gene set enrichment analysis: a knowledge-based approach for interpreting genome-wide expression profiles. Proc Natl Acad Sci USA 102(43):15545–15550. https://doi.org/10.1073/pnas.0506580102
23. Sokolowski E, Turina CB, Kikuchi K, Langenau DM, Keller C (2014) Proof-of-concept rare cancers in drug development: the case for rhabdomyosarcoma. Oncogene 33(15):1877–1889. https://doi.org/10.1038/onc.2013.129
24. Lalloo AK, Luo FR, Guo A, Paranjpe PV, Lee SH, Vyas V, Rubin E, Sinko PJ (2004) Membrane transport of camptothecin: facilitation by human P-glycoprotein (ABCB1) and multidrug resistance protein 2 (ABCC2). BMC Med 2:16. https://doi.org/10.1186/1741-7015-2-16
25. Lin F, Marchetti S, Pluim D, Iusuf D, Mazzanti R, Schellens JH, Beijnen JH, van Tellingen O (2013) Abcc4 together with abcb1 and abcg2 form a robust cooperative drug efflux system that restricts the brain entry of camptothecin analogues. Clin Cancer Res 19(8):2084–2095. https://doi.org/10.1158/1078-0432.CCR-12-3105
26. Rokita JL, Rathi KS, Cardenas MF, Upton KA, Jayaseelan J, Cross KL, Pfeil J, Egolf LE, Way GP, Farrel A, Kendsersky NM, Patel K, Gaonkar KS, Modi A, Berko ER, Lopez G, Vaksman Z, Mayoh C, Nance J, McCoy K, Haber M, Evans K, McCalmont H, Bendak K, Böhm JW, Marshall GM, Tyrrell V, Kalletla K, Braun FK, Qi L, Du Y, Zhang H, Lindsay HB, Zhao S, Shu J, Baxter P, Morton C, Kurmashev D, Zheng S, Chen Y, Bowen J, Bryan AC, Leraas KM, Coppens SE, Doddapaneni H, Momin Z, Zhang W, Sacks GI, Hart LS, Krytska K, Mosse YP, Gatto GJ, Sanchez Y, Greene CS, Diskin SJ, Vaske OM, Haussler D, Gastier-Foster JM, Kolb EA, Gorlick R, Li XN, Reynolds CP, Kurmasheva RT, Houghton PJ, Smith MA, Lock RB, Raman P, Wheeler DA, Maris JM (2019) Genomic profiling of childhood tumor patient-derived xenograft models to enable rational clinical trialdesign. Cell Rep 29(6):1675–1689.e9. https://doi.org/10.1016/j.celrep.2019.09.071
27. Ma X, Liu Y, Liu Y, Alexandrov LB, Edmonson MN, Gawad C, Zhou X, Li Y, Rusch MC, Easton J, Huether R, Gonzalez-Pena V, Wilkinson MR, Hermida LC, Davis S, Sioson E, Pounds S, Cao X, Ries RE, Wang Z, Chen X, Dong L, Diskin SJ, Smith MA, Guidry Auvil JM, Meltzer PS, Lau CC, Perlman EJ, Maris JM, Meshinchi S, Hunger SP, Gerhard DS, Zhang J (2018) Pan-cancer genome and transcriptome analyses of 1,699 paediatric leukaemias and solid tumours. Nature 555(7696):371–376. https://doi.org/10.1038/nature25795
28. Chen Y, Takita J, Choi YL, Kato M, Ohira M, Sanada M, Wang L, Soda M, Kikuchi A, Igarashi T, Nakagawara A, Hayashi Y, Mano H, Ogawa S (2008) Oncogenic mutations of ALK kinase in neuroblastoma. Nature 455(7215):971–974. https://doi.org/10.1038/nature07399
29. Janoueix-Lerosey I, Lequin D, Brugieres L, Ribeiro A, de Pontual L, Combaret V, Raynal V, Puisieux A, Schleiermacher G, Pierron G, Valteau-Couanet D, Frebourg T, Michon J, Lyonnet S, Amiel J, Delattre O (2008) Somatic and germline activating mutations of the ALK kinase receptor in neuroblastoma. Nature 455(7215):967–970. https://doi.org/10.1038/nature07398
30. Eleveld TF, Oldridge DA, Bernard V, Koster J, Colmet Daage L, Diskin SJ, Schild L, Bentahar NB, Bellini A, Chicard M, Lapouble E, Combaret V, Legoix-Ne P, Michon J, Pugh TJ, Hart LS, Rader J, Attiyeh EF, Wei JS, Zhang S, Naranjo A, Gastier-Foster JM, Hogarty MD, Asgharzadeh S, Smith MA, Guidry Auvil JM, Watkins TB, Zwijnenburg DA, Ebus ME, van Sluis P, Hakkert A, van Wezel E, van der Schoot CE, Westerhout EM, Schulte JH, Tytgat GA, Dolman ME, Janoueix-Lerosey I, Gerhard DS, Caron HN, Delattre O, Khan J, Versteeg R, Schleiermacher G, Molenaar JJ, Maris JM (2015) Relapsed neuroblastomas show frequent RAS-MAPK pathway mutations. Nat Genet 47(8):864–871. https://doi.org/10.1038/ng.3333
31. Kieran MW (2014) Targeted treatment for sonic hedgehog-dependent medulloblastoma. Neuro Oncol 16(8):1037–1047. https://doi.org/10.1093/neuonc/nou109
32. Kieran MW (2014) Targeting BRAF in pediatric brain tumors. Am Soc Clin Oncol Educ Book 34:e436–e440. https://doi.org/10.14694/EdBook_AM.2014.34.e436
33. Banerjee A, Jakacki RI, Onar-Thomas A, Wu S, Nicolaides T, Young Poussaint T, Fangusaro J, Phillips J, Perry A, Turner D, Prados M, Packer RJ, Qaddoumi I, Gururangan S, Pollack IF, Goldman S, Doyle LA, Stewart CF, Boyett JM, Kun LE, Fouladi M (2017) A phase I trial of the MEK inhibitor selumetinib (AZD6244) in pediatric patients with recurrent or refractory low-grade glioma: a Pediatric Brain Tumor Consortium (PBTC) study. Neuro Oncol 19(8):1135–1144. https://doi.org/10.1093/neuonc/now282
34. Fangusaro J, Onar-Thomas A, Young Poussaint T, Wu S, Ligon AH, Lindeman N, Banerjee A, Packer RJ, Kilburn LB, Goldman S, Pollack IF, Qaddoumi I, Jakacki RI, Fisher PG, Dhall G, Baxter P, Kreissman SG, Stewart CF, Jones DTW, Pfister SM, Vezina G, Stern JS, Panigrahy A, Patay Z, Tamrazi B, Jones JY, Haque SS, Enterline DS, Cha S, Fisher MJ, Doyle LA, Smith M, Dunkel IJ, Fouladi M (2019) Selumetinib in paediatric patients with BRAF-aberrant or neurofibromatosis type 1-associated recurrent, refractory, or progressive low-grade glioma: a multicentre, phase 2 trial. Lancet Oncol 20(7):1011–1022. https://doi.org/10.1016/S1470-2045(19)30277-3
35. Ooms AH, Gadd S, Gerhard DS, Smith MA, Guidry Auvil JM, Meerzaman D, Chen QR, Hsu CH, Yan C, Nguyen C, Hu Y, Ma Y, Zong Z, Mungall AJ, Moore RA, Marra MA, Huff V, Dome JS, Chi YY, Tian J, Geller JI, Mullighan CG, Ma J, Wheeler DA, Hampton OA, Walz AL, van den Heuvel-Eibrink MM, de Krijger RR, Ross N, Gastier-Foster JM, Perlman EJ (2016) Significance of TP53 mutation in wilms tumors with diffuse anaplasia: a report from the children's oncology group. Clin Cancer Res 22(22):5582–5591. https://doi.org/10.1158/1078-0432.CCR-16-0985
36. Bardeesy N, Falkoff D, Petruzzi MJ, Nowak N, Zabel B, Adam M, Aguiar MC, Grundy P, Shows T, Pelletier J (1994) Anaplastic Wilms' tumour, a subtype displaying poor prognosis, harbours p53 gene mutations. Nat Genet 7(1):91–97. https://doi.org/10.1038/ng0594-91
37. Long GV, Hauschild A, Santinami M, Atkinson V, Mandala M, Chiarion-Sileni V, Larkin J, Nyakas M, Dutriaux C, Haydon A, Robert C, Mortier L, Schachter J, Schadendorf D, Lesimple T, Plummer R, Ji R, Zhang P, Mookerjee B, Legos J, Kefford R, Dummer R, Kirkwood JM (2017) Adjuvant dabrafenib plus trametinib in stage III BRAF-mutated melanoma. N Engl J Med 377(19):1813–1823. https://doi.org/10.1056/NEJMoa1708539
38. Fiskus W, Mitsiades N (2016) B-raf inhibition in the clinic: present and future. Annu Rev Med 67:29–43. https://doi.org/10.1146/annurev-med-090514-030732
39. Houdaihed L, Evans JC, Allen C (2017) Overcoming the road blocks: advancement of block copolymer micelles for cancer therapy in the clinic. Mol Pharm 14(8):2503–2517. https://doi.org/10.1021/acs.molpharmaceut.7b00188
40. Maeda H (2012) Macromolecular therapeutics in cancer treatment: the EPR effect and beyond. J Control Release 164(2):138–144. https://doi.org/10.1016/j.jconrel.2012.04.038

41. Gokduman K (2016) Strategies targeting DNA topoisomerase I in cancer chemotherapy: camptothecins, nanocarriers for camptothecins, organic non-camptothecin compounds and metal complexes. Curr Drug Targets 17(16):1928–1939
42. Kaufmann SH (1998) Cell death induced by topoisomerase-targeted drugs: more questions than answers. Biochim Biophys Acta 1400(1–3):195–211
43. Wagner LM (2015) Fifteen years of irinotecan therapy for pediatric sarcoma: where to next? Clin Sarcoma Res 5:20. https://doi.org/10.1186/s13569-015-0035-x
44. Metzger ML, Stewart CF, Freeman BB 3rd, Billups CA, Hoffer FA, Wu J, Coppes MJ, Grant R, Chintagumpala M, Mullen EA, Alvarado C, Daw NC, Dome JS (2007) Topotecan is active against wilms' tumor: results of a multi-institutional phase II study. J Clin Oncol 25(21):3130–3136. https://doi.org/10.1200/JCO.2007.10.9298
45. Furman WL, Stewart CF, Kirstein M, Kepner JL, Bernstein ML, Kung F, Vietti TJ, Steuber CP, Becton DL, Baruchel S, Pratt C (2002) Protracted intermittent schedule of topotecan in children with refractory acute leukemia: a pediatric oncology group study. J Clin Oncol 20(6):1617–1624. https://doi.org/10.1200/JCO.2002.20.6.1617
46. Daw NC, Anderson JR, Hoffer FA, Geller JI, Kalapurakal JA, Perlman EJ (2017) A phase 2 study of vincristine and irinotecan in metastatic diffuse anaplastic wilms tumor: results from the children's oncology group AREN0321 study. J Clin Oncol 32(suppl 15):10032
47. Palmerini E, Jones RL, Setola E, Picci P, Marchesi E, Luksch R, Grignani G, Cesari M, Longhi A, Abate ME, Paioli A, Szucs Z, D'Ambrosio L, Scotlandi K, Fagioli F, Asaftei S, Ferrari S (2018) Irinotecan and temozolomide in recurrent ewing sarcoma: an analysis in 51 adult and pediatric patients. Acta Oncol 57(7):958–964. https://doi.org/10.1080/0284186X.2018.1449250
48. Rose WC, Wild R (2004) Therapeutic synergy of oral taxane BMS-275183 and cetuximab versus human tumor xenografts. Clin Cancer Res 10(21):7413–7417. https://doi.org/10.1158/1078-0432.CCR-04-1045
49. Yoo E, Kim BU, Lee SY, Cho CH, Chung JH, Lee CH (2005) 53BP1 is associated with replication protein A and is required for RPA2 hyperphosphorylation following DNA damage. Oncogene 24(35):5423–5430. https://doi.org/10.1038/sj.onc.1208710
50. Houghton PJ, Stewart CF, Zamboni WC, Thompson J, Luo X, Danks MK, Houghton JA (1996) Schedule-dependent efficacy of camptothecins in models of human cancer. Ann N Y Acad Sci 803:188–201. https://doi.org/10.1111/j.1749-6632.1996.tb26388.x
51. Houghton PJ, Cheshire PJ, Hallman JC, Bissery MC, Mathieu-Boue A, Houghton JA (1993) Therapeutic efficacy of the topoisomerase I inhibitor 7-ethyl-10-(4-[1-piperidino]-1-piperidino)-carbonyloxy-camptothecin against human tumor xenografts: lack of cross-resistance in vivo in tumors with acquired resistance to the topoisomerase I inhibitor 9-dimethylaminomethyl-10-hydroxycamptothecin. Cancer Res 53(12):2823–2829
52. Stewart CF, Leggas M, Schuetz JD, Panetta JC, Cheshire PJ, Peterson J, Daw N, Jenkins JJ 3rd, Gilbertson R, Germain GS, Harwood FC, Houghton PJ (2004) Gefitinib enhances the antitumor activity and oral bioavailability of irinotecan in mice. Cancer Res 64(20):7491–7499. https://doi.org/10.1158/0008-5472.CAN-04-0096
53. Furman WL, Navid F, Daw NC, McCarville MB, McGregor LM, Spunt SL, Rodriguez-Galindo C, Panetta JC, Crews KR, Wu J, Gajjar AJ, Houghton PJ, Santana VM, Stewart CF (2009) Tyrosine kinase inhibitor enhances the bioavailability of oral irinotecan in pediatric patients with refractory solid tumors. J Clin Oncol 27(27):4599–4604. https://doi.org/10.1200/JCO.2008.19.6642
54. Grobner SN, Worst BC, Weischenfeldt J, Buchhalter I, Kleinheinz K, Rudneva VA, Johann PD, Balasubramanian GP, Segura-Wang M, Brabetz S, Bender S, Hutter B, Sturm D, Pfaff E, Hubschmann D, Zipprich G, Heinold M, Eils J, Lawerenz C, Erkek S, Lambo S, Waszak S, Blattmann C, Borkhardt A, Kuhlen M, Eggert A, Fulda S, Gessler M, Wegert J, Kappler R, Baumhoer D, Burdach S, Kirschner-Schwabe R, Kontny U, Kulozik AE, Lohmann D, Hettmer S, Eckert C, Bielack S, Nathrath M, Niemeyer C, Richter GH, Schulte J, Siebert R, Westermann F, Molenaar JJ, Vassal G, Witt H, Project IP-S, Project IM-S, Burkhardt B, Kratz CP, Witt O, van Tilburg CM, Kramm CM, Fleischhack G, Dirksen U, Rutkowski S, Fruhwald M, von Hoff K, Wolf S, Klingebiel T, Koscielniak E, Landgraf P, Koster J, Resnick AC, Zhang J, Liu Y, Zhou X, Waanders AJ, Zwijnenburg DA, Raman P, Brors B, Weber UD, Northcott PA, Pajtler KW, Kool M, Piro RM, Korbel JO, Schlesner M, Eils R, Jones DTW, Lichter P, Chavez L, Zapatka M, Pfister SM (2018) The landscape of genomic alterations across childhood cancers. Nature 555(7696):321–327. https://doi.org/10.1038/nature25480